# Terahertz generation from coherent optical phonons in a biased GaAs photoconductive emitter

Y. C. Shen, P. C. Upadhya, E. H. Linfield,* and H. E. Beere
*Cavendish Laboratory, University of Cambridge, Madingley Road, Cambridge CB3 0HE, United Kingdom*

A. G. Davies
*School of Electronic and Electrical Engineering, University of Leeds, Leeds LS2 9JT, United Kingdom*
(Received 19 November 2003; revised manuscript received 11 February 2004; published 28 June 2004)

Terahertz radiation, generated from a biased and asymmetrically excited low-temperature-grown GaAs photoconductive emitter, has been characterized with a 20-$\mu$m-thick ZnTe crystal using free-space electro-optic sampling. Pronounced coherent emission, originating from longitudinal optical phonon oscillations, has been observed, with a characteristic frequency of 8.7 THz and a decay time of 2.1 ps. In the frequency domain, the sharp spectral features from phonon oscillations superimpose on an ultrabroad (over 20 THz) response from the initial transient. Furthermore, a broad feature around 16 THz is observed, and interpreted as originating from the coherent plasmon-phonon coupled modes.

DOI: 10.1103/PhysRevB.69.235325 PACS number(s): 78.47.+p, 72.20.Jv, 72.30.+q, 73.20.Mf

The generation and detection of coherent optical phonons in semiconductors has been studied previously using both optical transient reflectivity measurements[1–6] and terahertz (THz) emission spectroscopy.[7–10] In a polar material, such as GaAs, the electric fields interact with both electrons and optical phonons. Thus after optical excitation, photogenerated carriers can be separated by an electric field, creating electronic polarization, and this polarization, in turn, partially screens the electric field and causes the lattice to oscillate at phonon frequencies. Coherent longitudinal-optical (LO) phonon oscillations in bulk GaAs were first observed through electro-optic modulations of the transient reflectivity.[1] Theoretical investigations[11] predict that coherent LO phonon modes excited in a finite-size volume produce oscillations of macroscopic dielectric polarization, and this is expected to emit electromagnetic radiation at the phonon frequency. Indeed, THz radiation emitted by coherent phonons has been observed in Te, PbTe, and CdTe.[7,8] However, THz radiation originating from coherent phonon oscillations has not been observed in GaAs photoconductive emitters, despite the fact that photoconductive emitters are the most efficient device for converting visible/near-IR laser pulses to THz radiation[12,13] and have been widely used for THz spectroscopy and imaging.

We report a time-resolved observation of THz emission originating from the macroscopic polarization associated with coherent LO phonon oscillations in biased low-temperature- (LT-) grown GaAs photoconductive emitters. The radiation was detected using free-space electro-optic sampling,[14,15] which allowed the direct measurement of the amplitude and phase of the coherent electromagnetic radiation emitted after pulsed optical excitation. The experimental results give insight into the dynamics of photogenerated carriers and phonon oscillations in semiconductors.

The experimental apparatus for coherent generation and detection of THz radiation has been reported previously.[16] In brief, a Ti:sapphire laser provides visible/near-infrared pulses of 12 fs duration at a center wavelength of 790 nm with a repetition rate of 76 MHz. The output is split into two parts: a 250 mW beam is used for THz generation and a 25 mW beam serves as the probe beam for electro-optic detection using a 20-$\mu$m-thick (110) ZnTe crystal glued onto a 1-mm-thick wedged (100) ZnTe crystal. Note that for generating ultrabroadband THz radiation, the pump laser beam was tightly focused to a 40-$\mu$m-diameter spot on the edge of one of the two NiCr/Au electrodes of the biased LT-GaAs emitter [Fig. 1(a) inset], and the LT-GaAs used had a carrier recombination lifetime of 0.4 ps. Furthermore, in contrast to previous experiments, where the THz radiation was collected forwards (that is, after being transmitted through the GaAs substrate), the THz radiation was collected backwards (in the direction of the reflected pump laser beam). As will be shown later, this arrangement minimizes the absorption and dispersion of the THz pulses in the GaAs substrate. In all measurements, the variable delay stage, which provides the time delay between the THz pulse and the probe pulse, was scanned over a distance of 2 mm, providing a spectral resolution of 75 GHz (2.5 $cm^{-1}$). The whole apparatus was enclosed in a vacuum-tight box, which was purged with dry nitrogen gas to reduce the effects of water vapor absorption. All measurements were performed at room temperature.

Figure 1(a) shows a typical temporal THz wave form from the photoconductive emitter, with Fig. 1(b) showing the corresponding frequency spectrum. In the time domain, pronounced fast phonon oscillations are immediately visible after the initial transient. These represent an observation of THz radiation from optical phonon oscillations in a biased photoconductive emitter. In the frequency domain, the individual phonon spectral features superimpose with an ultrabroad response from the initial transient. The coherent plasmon-phonon coupled modes are responsible for a small broad feature around 16 THz [marked with an arrow in Figs. 1(b) and 2]. Note that frequency components over 20 THz are observed, and this has been previously used to obtain ultrabroadband THz spectra.[16]

The main positive peak of the pulse has a rise time (from 10 to 90 % of the peak height) of 60 fs, and a much shorter fall time of 13 fs. The electric field applied to the photoconductive emitter accelerates the electrons and holes and this ballistic acceleration leads to the positive peak in THz emis-

 

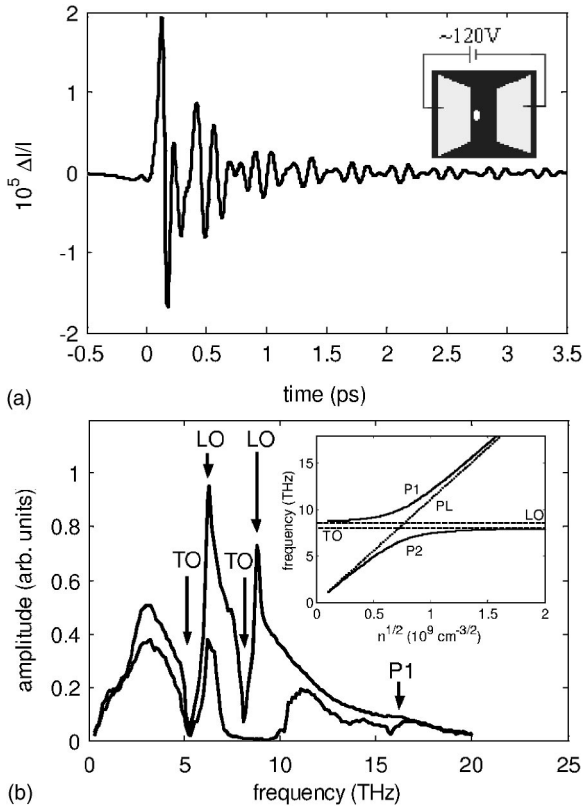


FIG. 1. (a) The temporal THz wave form and (b) its corresponding Fourier-transform amplitude spectrum (upper trace), together with the spectrum measured after being transmitted through a 0.53-mm-thick GaAs wafer (lower trace). The arrows mark spectral features corresponding to the TO and LO phonons of ZnTe ($\nu_{TO} \equiv 5.3$ THz; $\nu_{LO} \equiv 6.2$ THz) and GaAs ($\nu_{TO} \equiv 8.06$ THz; $\nu_{LO} \equiv 8.76$ THz), together with the coupled plasmon-phonon mode of GaAs (P1). Inset of (a): Schematic geometry of the electrodes (0.4 mm gap) used in the biased GaAs photoconductive emitter. The white spot ($\sim 40\ \mu$m diameter) indicates the position of the asymmetric laser excitation. Inset of (b): Density dependence of coupled plasmon-phonon mode frequencies (upper branch: P1; lower branch: P2) calculated for GaAs parameters ($\varepsilon_0 = 12.9$, $\varepsilon_\infty = 10.9$, $\nu_{LO} = 8.76$ THz, $\nu_{TO} = 8.06$ THz, and $\mu = 0.06 m_0$). Dashed and dotted lines represent GaAs TO phonon, LO-phonon and plasmon (PL) frequencies, respectively.

sion. The resulting space-charge field, however, screens the electrostatic field. This reduces the driving force on the carriers, causing a reduced carrier acceleration. In addition, it should be noted that the photoconductive emitter is biased at 120 V, and the spatial distribution of the resulting electric field is highly nonuniform, with 80% of the field being concentrated within a $\sim 20\ \mu$m region near the anode.[12] Therefore, a high field (over 30 kV/cm) is expected in this region, which is well above the Gunn threshold (5.3 kV/cm) of GaAs.[9] As the photogenerated carriers gain momentum in the strong external field, they are therefore able to scatter to the side valleys ($\Gamma$ to $L$ splitting in GaAs: 330 meV). This explains the strong and fast deceleration observed in our experiments as a fall in THz emission.

In addition to the initial transients caused by the free carrier acceleration and deceleration, the THz signal also demonstrates the oscillation of ions in the polar crystal lattice. This coherent oscillation is initiated by the motion of the photogenerated carriers, since the displacement of these electron-hole pairs in the presence of an external field leads to a small but ultrafast change of the internal electric field. The polar crystal lattice thus becomes excited impulsively as the ions accelerate towards their new equilibrium positions.[9] As a result, a strong THz component, oscillating at the LO phonon frequency, is superimposed on the main pulse.

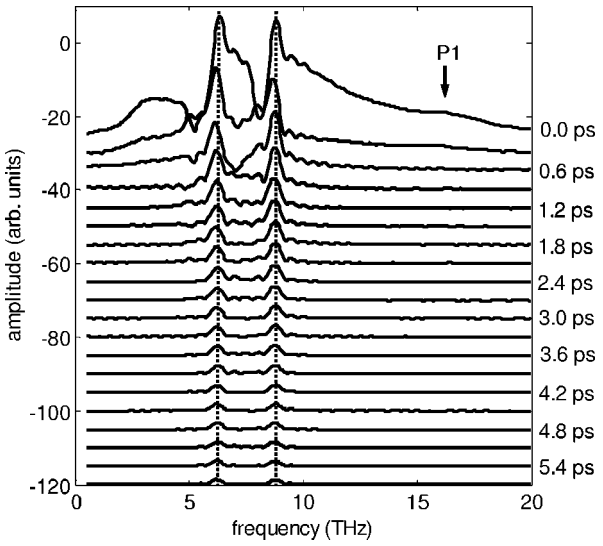


FIG. 2. The time-partitioned Fourier transform of the THz data from Fig. 1. The time interval between two adjacent curves is 0.3 ps, with the time on the right-hand axis being the start of the 2 ps partitioning interval. Two dotted lines correspond to frequencies 6.2 and 8.7 THz, and the arrow (P1) indicates the broad feature originating from coupled plasmon-phonon modes.

In order to study the dynamics of the observed phonon oscillations, we calculated the time-partitioned Fourier transform of the THz signal in a confined 2 ps time window. As shown in Fig. 2, all time-partitioned Fourier transforms are dominated by two peaks at fixed frequencies of 6.2 and 8.7 THz, and almost all other frequency components diminish within the first 0.3 ps after excitation. Furthermore, the amplitudes of the frequency components at 6.2 and 8.7 THz decrease at later times. The relaxation time of the oscillations can be quantitatively determined by fitting the measured time-domain THz signal, with an expression based on two exponentially decaying sine waves

$$E_{\mathrm{THz}}(t) = A_1 \sin(2\pi\nu_1 t + \phi_1) e^{-t/\tau_1} + A_2 \sin(2\pi\nu_2 t + \phi_2) e^{-t/\tau_2}.$$

As shown in Fig. 3, the agreement between the fitted and the measured THz signals is exceptionally good. The best-fit values of $\nu_1$ and $\nu_2$ are 6.2 and 8.7 THz, with relaxation times of 3.0 and 2.1 ps, respectively. We attribute the peak at 8.7 THz in Fig. 1(b) as originating from LO phonon oscillations in GaAs. The 2.1 ps relaxation time of this mode depends on the momentum and phonon dephasing via anharmonic interactions. This value is close to the 1.5 ps measured in reflectivity measurements of a GaAs photoconductive emitter,[5] but is smaller than the 5 ps reported for GaAs

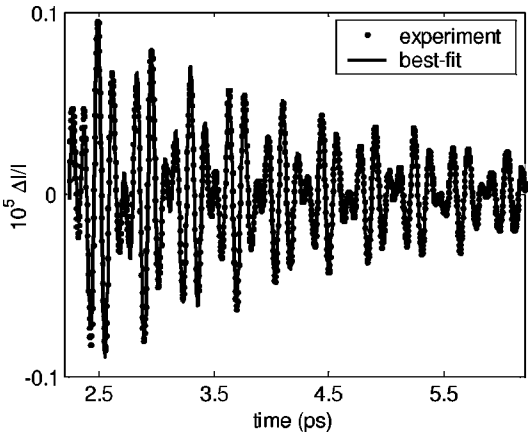


FIG. 3. The measured (points) and calculated (curve) temporal THz wave form between 2.3–6.3 ps. Note that the phonon oscillations can be seen immediately after the initial transient [see Fig. 1(a)], and extend over 8.0 ps, although for clarity, only a restricted interval is shown here.

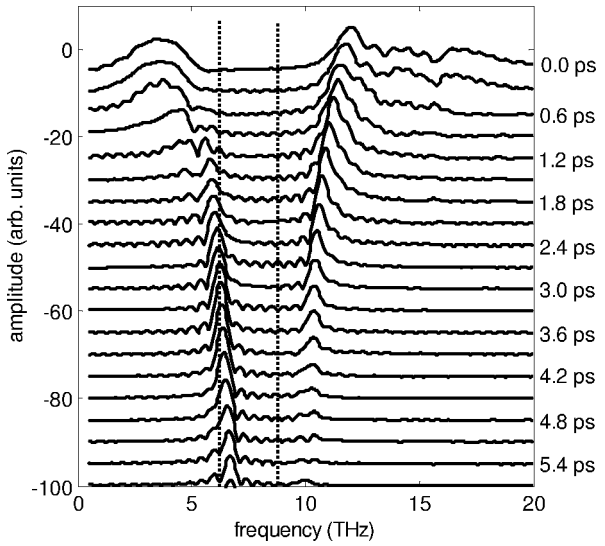


FIG. 4. The time-partitioned Fourier transform of the THz signal measured after being transmitted through a 0.53-mm-thick GaAs wafer. The time interval between two adjacent curves is 0.3 ps, with the time on the righthand axis being the start of the 2 ps partitioning interval. Two dotted lines correspond to frequencies 6.2 and 8.7 THz.

*p-i-n* diodes.[9] In explanation, the maximum carrier concentration in our measurement ($\sim 3\times 10^{18}$ cm$^{-3}$) is close to that of Cummings *et al.*[6] ($5.6\times 10^{18}$ cm$^{-3}$), but much larger than that of Leitenstorfer *et al.*[9] ($5\times 10^{14}$ cm$^{-3}$), suggesting that the relaxation time of the photogenerated carriers is carrier concentration dependent. We note that in their transient reflectivity measurements, Cummings *et al.*[5] observed both transverse-optical (TO) phonon and LO phonon oscillations in a biased GaAs photoconductive emitter. In our experiments we observed a spectral peak at the LO oscillation frequency and a spectral dip at the TO oscillation frequency. The spectral dip at 8.1 THz can be explained by the reduced coupling efficiency of THz radiation to free space owing to the large value of the refractive index of GaAs near the TO phonon frequency ($\nu_{\mathrm{TO}}=8.06$ THz).[8] We note that THz radiation generated from LO phonons (spectral peak at 8.7 THz) is further enhanced by the increased coupling efficiency of THz radiation from the GaAs substrate to free space owing to the small value of the refractive index of GaAs near the LO frequency.[8,17] The spectral dip at 5.3 THz and the peak at 6.2 THz arise from the response of the ZnTe detector ($\nu_{\mathrm{TO}}=5.3$ THz; $\nu_{\mathrm{LO}}=6.2$ THz).[14,15]

It is interesting that we observed the coupled plasmon-phonon modes in a biased photoconductive emitter [a broad feature around 16 THz, see Figs. 1(b) and 2]. In polar materials such as GaAs, where LO phonons and plasmons combine into coupled plasmon-phonon modes, one can expect both modes to be excited by ultrafast screening. The frequency of the LO phonon mode is carrier density independent while the frequency of the coupled plasmon-phonon modes [$P_1$, $P_2$ in the inset Fig. 1(b)] are density dependent. One would expect to see only the density-independent LO-phonon oscillations because the density-dependent plasmon-phonon coupled modes are smoothed out by averaging over the spatial distribution of the photogenerated carrier density.[11] As a result, oscillations at LO phonon frequencies have been reported in all previous studies,[1–10] while the frequency-dependent plasmon-phonon coupled modes have only been observed for the case of *n*-doped materials.[4,10] In our experiment, we directly probe THz radiation emitted from the GaAs photoconductive emitter, which strongly depends on both the photogenerated carrier density and the local electric field.[18] Although the photocarrier distribution generated by the 40-$\mu$m-diameter laser spot is nonuniform, the emitted signal is dominated by the relatively uniform carrier distribution across the 20-$\mu$m-wide high electric field region. Consequently, this leads to the observation of radiation at 16 THz originating from coupled plasmon-phonon modes.

It should be pointed out that the observation of THz radiation from coupled plasmon-phonon modes has important implications for practical applications. As shown in the inset of Fig. 1(b), the frequency of plasmon oscillations, and that of the upper branch of the coupled plasmon-phonon modes in GaAs, is proportional to the square root of the free carrier density. Therefore one can in principle generate efficiently in the mid-IR range (e.g., $\sim$30 THz) by increasing the photogenerated carrier density (e.g., $\sim 8\times 10^{18}$ cm$^{-3}$), either by increasing the pump laser power or reducing the laser spot size in appropriately miniaturized and optimized photoconductive emitters. Such photoconductive emitters will find use in pump-probe studies in both the mid-IR and far-IR frequency ranges.[19,20]

Figure 1(b) also shows the amplitude spectrum of the THz signal measured after being transmitted through a 0.53-mm-thick semi-insulating (SI) GaAs wafer. As expected, the measured spectrum [lower trace of Fig. 1(b)] shows strong THz absorption owing to single- and multiphonon bands. To further understand the phonon dynamics of GaAs, we once again calculated the time-partitioned Fourier transform of the THz signal in a confined time window of 2 ps. As shown in Fig. 4, after passing through the GaAs wafer, the different frequency components in the THz pulse arrive at different

delay times, with frequency components closer to the reststrahlen band arriving at later times. The frequency components near the reststrahlen band region are thus stored in the material for some time before being radiated. These experimental results (Fig. 4) are fully replicated by numerical simulations (not shown here) using classical electromagnetic wave theory, taking into account the incident THz pulse shape and the frequency-dependent complex dielectric constant of GaAs.

In conclusion, we have investigated the generation of THz radiation in GaAs photoconductive devices. We observed THz emission originating from the macroscopic polarization associated with coherent LO phonon oscillations in biased LT-GaAs photoconductive emitters. These oscillations are at the LO phonon frequency of GaAs and have a relaxation time of 2.1 ps. We also found that the coupled plasmon-phonon modes contribute to the emitted THz radiation. The ultrabroadband (over 20 THz) nature of the THz radiation generated in photoconductive emitters can be used for THz spectroscopy and for studying the dynamics of solids.

This work was supported by the EPSRC and Toshiba Research Europe, Ltd. (EHL).

*Email address: ehl10@cam.ac.uk

[1] G. C. Cho, W. Kütt, and H. Kurz, Phys. Rev. Lett. **65**, 764 (1990).
[2] T. Pfeifer, W. Kütt, H. Kurz, and R. Scholz, Phys. Rev. Lett. **69**, 3248 (1992).
[3] T. K. Cheng, S. D. Brorson, A. S. Kazeroonian, J. S. Moodera, G. Dresselhaus, M. S. Dresselhaus, and E. P. Ippen, Appl. Phys. Lett. **57**, 1004 (1990); **59**, 1923 (1991).
[4] G. C. Cho, T. Dekorsy, H. J. Bakker, R. Hövel, and H. Kurz, Phys. Rev. Lett. **77**, 4062 (1996).
[5] M. D. Cummings, J. F. Holzman, and Y. Elezzabi, Appl. Phys. Lett. **78**, 3535 (2001).
[6] M. Hase, M. Kitajima, S. I. Nakashima, and K. Mizoguchi, Phys. Rev. Lett. **88**, 067401 (2002).
[7] T. Dekorsy, H. Auer, C. Waschke, H. J. Bakker, H. G. Roskos, H. Kurz, V. Wagner, and P. Grosse, Phys. Rev. Lett. **74**, 738 (1995); Phys. Rev. B **53**, 4005 (1996).
[8] M. Tani, R. Fukasawa, H. Abe, K. Sakai, and S. Nakashima, J. Appl. Phys. **83**, 2473 (1998).
[9] A. Leitenstorfer, S. Hunsche, J. Shah, M. C. Nuss, and W. H. Knox, Phys. Rev. Lett. **82**, 5140 (1999); Phys. Rev. B **61**, 16642 (2000).
[10] M. P. Hasselbeck, D. Stalnaker, L. A. Schlie, T. J. Rotter, A. Stintz, and M. Sheik-Bahae, Phys. Rev. B **65**, 233203 (2002).
[11] A. V. Kuznetsov and C. J. Stanton, Phys. Rev. B **51**, 7555 (1995).
[12] I. Brener, D. Dykaar, A. Frommer, L. N. Pfeiffer, J. Lopata, J. Wynn, K. West, and M. C. Nuss, Opt. Lett. **21**, 1924 (1996).
[13] G. Zhao, R. N. Schouten, N. van der Valk, W. Th. Wenckebach, and P. C. M. Planken, Rev. Sci. Instrum. **73**, 1715 (2002).
[14] Q. Wu and X.-C. Zhang, Appl. Phys. Lett. **70**, 1784 (1997).
[15] A. Leitenstorfer, S. Hunsche, J. Shah, M. C. Nuss, and W. H. Knox, Appl. Phys. Lett. **74**, 1516 (1999).
[16] Y. C. Shen, P. C. Upadhya, E. H. Linfield, H. E. Beere, and A. G. Davies, Appl. Phys. Lett. **83**, 3117 (2003).
[17] G. C. Cho, P. Y. Han, X.-C. Zhang, and H. J. Bakker, Opt. Lett. **25**, 1609 (2000).
[18] P. Uhd Jepsen, R. H. Jacobsen, and S. R. Keiding, J. Opt. Soc. Am. B **13**, 2424 (1996).
[19] R. Huber, F. Tauser, A. Brodschelm, M. Bichler, G. Abstreiter, and A. Leitenstorfer, Nature (London) **414**, 286 (2001).
[20] A. H. Xie, A. F. G. van der Meer, and R. H. Austin, Phys. Rev. Lett. **88**, 018102 (2002).